Meteorol. Atmos. Phys. 71, 169–188 (1999)

Meteorology
and Atmospheric
Physics

[1]Meteorology Group, Departament de Física, Universitat de les Illes Balears, Palma de Mallorca, Spain
[2]IMEDEA, UIB-CSIC, Palma de Mallorca, Spain
[3]Instituto Nacional de Meteorología, Madrid, Spain
[4]Departament de Física i Enginyeria Nuclear, Universitat Politècnica de Catalunya, Vilanova i la Geltrú, Barcelona, Spain

A Case of Convection Development over the Western Mediterranean Sea: A Study through Numerical Simulations

V. Homar[1], **C. Ramis**[1], **R. Romero**[1], **S. Alonso**[1,2], **J. A. García-Moya**[3], and **M. Alarcón**[4]

With 21 Figures

Received March 2, 1999

Summary

A convective case producing heavy precipitation in the western Mediterranean region, characterized by pronounced upper level forcing and main rainfall over the sea, is studied. On the day of the event (September 28th, 1994), more than 140 mm of precipitation were recorded in coastal lands of eastern Spain, and 180 mm were estimated over the sea with radar data. Synoptically, the case appears to combine warm and moist easterly advection at low levels, typically observed in torrential rainfall events of the region, with a less common strong upper level dynamical forcing. A set of mesoscale numerical simulations using the Hirlam model is performed to investigate the mechanisms responsible for the convection development, and to assess the influence of the orography on the rainfall field. Model output diagnosis indicates that in addition to the lower level forcing, a two-jets interaction is decisive for the triggering and driving of the convection during the event. Moreover, a non-topographic simulation reveals a relatively weak influence of the orography on this event when compared with other similar heavy precipitation cases in eastern Spain. Previous studies have shown an orographic influence of more than 90% on the rainfall whereas in this case about 50% of the precipitation over the area is attributed to the orographic forcing. The study is extended with an analysis of the individual effects of the Atlas and Iberian Peninsula, by means of a factor separation technique. It is shown that the Atlas range induces a redistribution of the precipitation over the Mediterranean, whereas local enhancements can be attributed to the Iberian topography.

1. Introduction

The afternoon of 28th and the early morning of September 29th 1994, an important rainfall event occurred over the western Mediterranean region (Fig. 1). The analized field of total precipitation recorded over the Spanish coastal lands during the 28th is depicted in Fig. 2. The rain affected mainly the region of Valencia, with maxima up to 140 mm, and the Balearic Islands, with a peak up to 170 mm over Mallorca. Serious damages in some agricultural and touristic areas occurred. Conversely, the Andalusia (to the southwest) and Catalonia (to the north) regions did not recorded any significant precipitation during the event.

Spanish Mediterranean area is usually affected by torrential (more than 100 mm/day) rainfall events (Llasat, 1987; García-Dana et al., 1982; Ramis et al., 1994; among others). In fact, many of the observatories of Catalonia, Valencia, Murcia and Andalusia have recorded daily rainfalls exceeding 200 mm as shown by Font (1983). There are some exceptional examples as the case occurred over Gandía (Valencia), where more than 800 mm in 24 hours were recorded. It has been shown that torrential events occur once or twice a year on average over

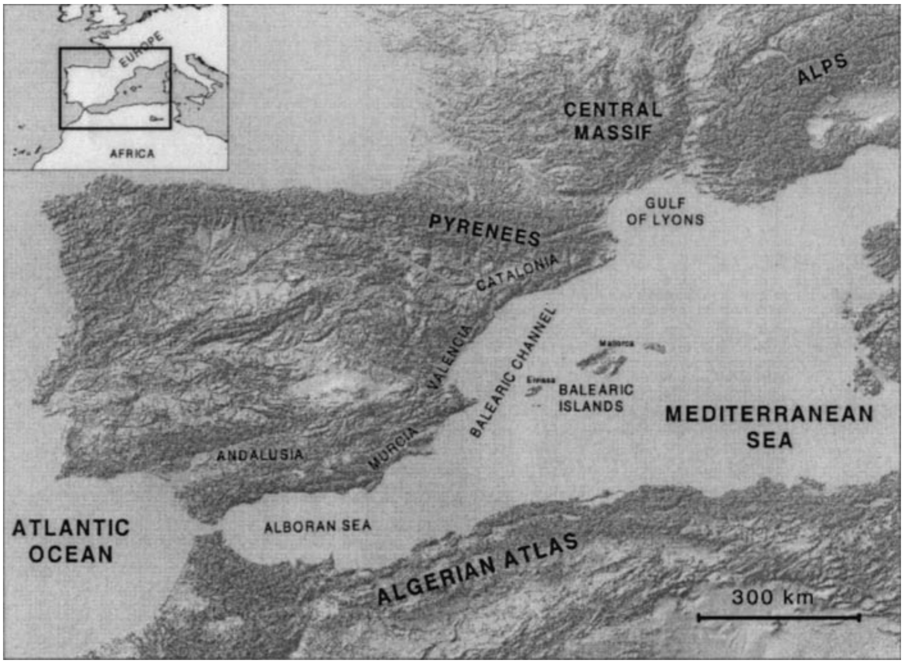

Fig. 1. The western Mediterranean area. The map includes the names of places referred to in the text

Valencia (Romero et al., 1999), normally in autumn, producing serious economic loses by the associated flash floods, mainly on the countryside.

Several studies using Meteosat imagery have led to the conclusions that deep convection, organised as mesoscale convective systems, is usually the responsible for the flash floods in Mediterranean Spain (e.g., Doswell III et al., 1998; Riosalido, 1990). The leading roles of the orography and the sea surface latent-heat flux have been demonstrated through numerical studies. The enclosing orography of the western Mediterranean Sea (notably Atlas, Pyrenees and Alps) usually interacts with the synoptic flux, modifying the circulation and generating mesoscale disturbances that force and focuse the convection in upslope zones. Moreover, sea surface temperature during autumn is higher than the temperature of the overlying air, being a good source of heat and moisture for the convective systems (Ramis et al., 1998).

Although a greater attention is paid to torrential rainfall over western Mediterranean coastal lands (due to social and economical impact), a significant number of events occur over the sea, affecting in some cases the Balearic Islands (e.g., Ramis et al., 1986). The case presented here was characterized by a convective development over the sea that evolved northwards as shown by Meteosat images (Fig. 3). The convection began early (0600 UTC) on September 28th over the Alboran Sea (Fig. 3a), and could be identified during more than 30 h. Two main convective systems can be identified in Fig. 3b, the western one being the responsible for the precipitation over Murcia and Valencia depicted in Fig. 2. This western convective system also released an important amount of precipitation over the sea, since three evident centers can be identified over the Balearic channel from the radar estimated 24 h rainfall (Fig. 4). The fact that the convective system started and followed its life cycle over the sea is an interesting issue, suggesting that the triggering and driving mechanisms contained none or weak direct orographic contribution. A priori, it seems to be a case mostly controlled by dynamical forcing and weakly influenced by orography.

The aim of this work is to investigate the factors responsible for the heavy rainfall observed, to determine what fraction of precipitation is due to pure dynamical forcing, and what is associated with the orography. In previous case studies of torrential rainfall over eastern Spain, more than 90% of the rainfall had an orographic origin (Romero et al., 1997; Ramis et al., 1998). This study is focused on diagnosis of mesoscale model outputs towards an identification of dynamical and thermodynamical "ingredients"

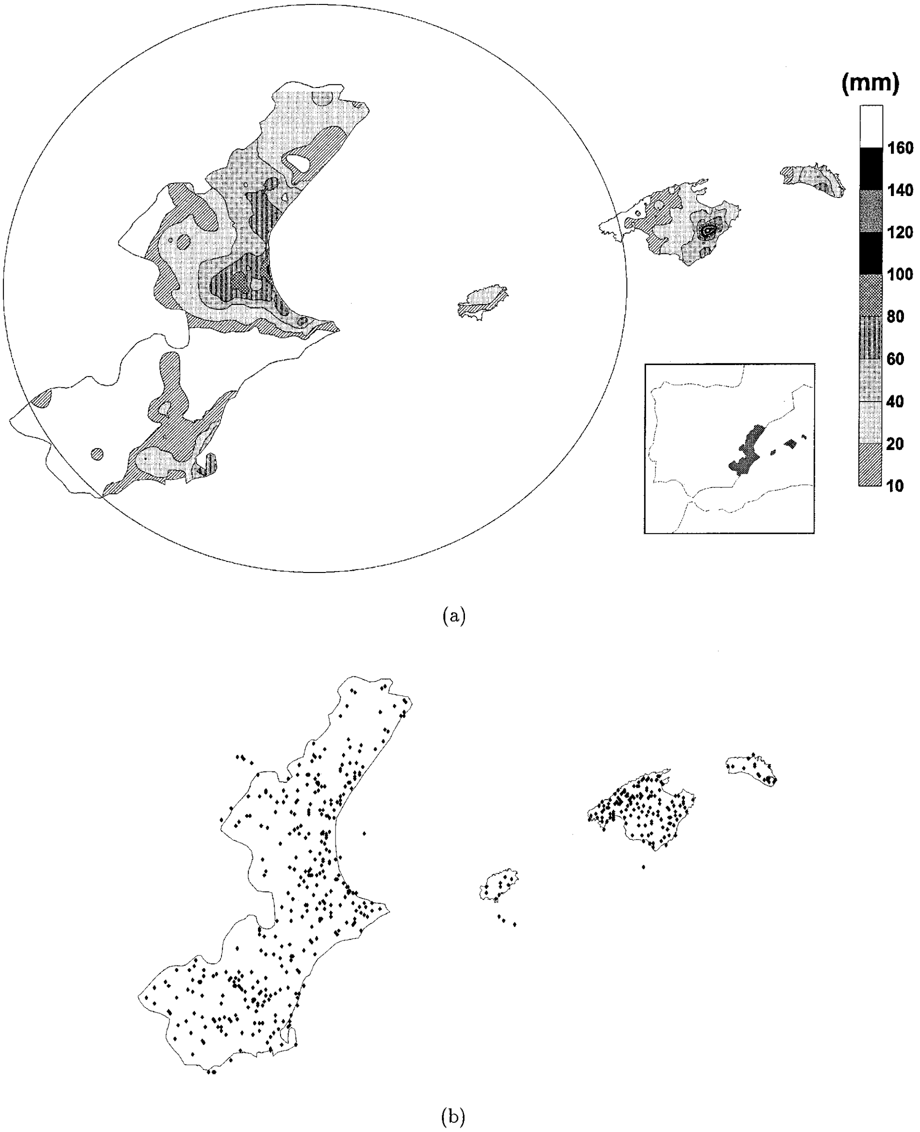

Fig. 2. a) Analysis of the recorded precipitation (mm) in Valencia, Murcia and Balearic Islands for the 24 h period from 0700 UTC September 28th to 0700 UTC September 29th, 1994. Circle indicates the coverage area of the Valencia radar (Fig. 4). b) Location of the raingauge stations used for the analysis

for convection development (Doswell III et al., 1996). This approach has been already used in previous studies of flash flood events in the western Mediterranean (see e.g., Ramis et al., 1998).

Section 2 provides a more extended overview of the case, using synoptic analysis, Meteosat imagery and radar information. The numerical model used is explained in Sect. 3. Section 4 presents the simulations: a complete simulation is analysed with the aim of validating the model run and assessing its diagnostic information; then non-topographic simulations are presented to quantify the orographic influence in this case. At the end, Sect. 5 presents the conclusions.

2. Overview of the Case

2.1 Synoptic Situation

Data from the 0.75° latitude-longitude ECMWF analyses at standard pressure levels have been used for the synoptic overview of the case. The meteorological situation at low levels on 1200 UTC September 28th is characterized by a large low over North Africa together with an anticyclon over the Atlantic Ocean, extending towards Central Europe. Both structures produce general easterly circulation over the western Mediterranean (see Fig. 5a, for 925 hPa). The temperature at those levels is mostly influenced by land

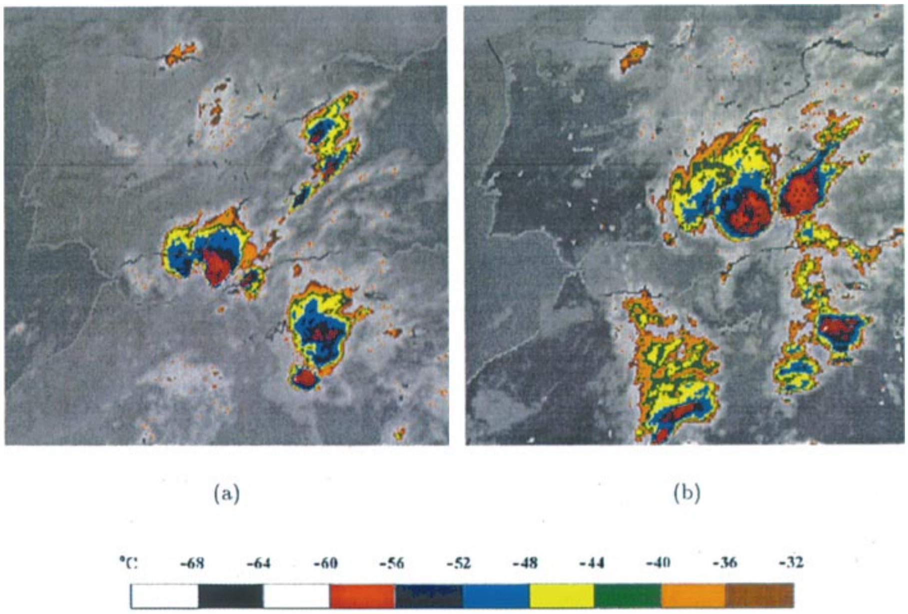

Fig. 3. Meteosat infrared images at a) 0600 UTC, b) 1100 UTC September 28th, 1994. Colours show cloud top temperature in °C

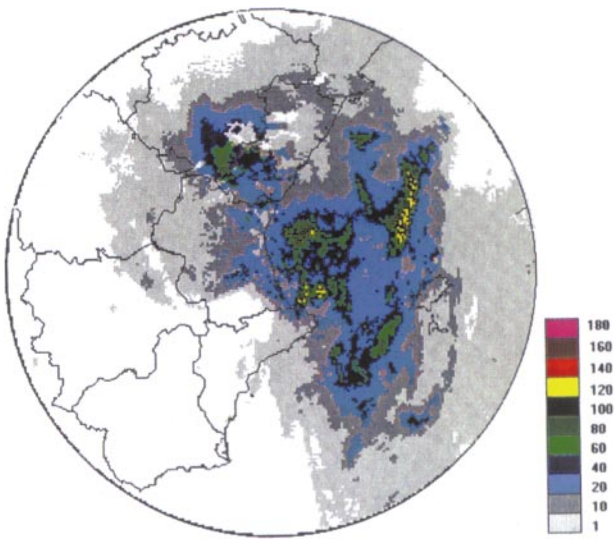

Fig. 4. Radar estimation of accumulated precipitation (mm) for the period from 0700 UTC 28th to 0700 UTC 29th September 1994

distribution, with warm areas over Africa and the Iberian Peninsula. Such circulation and thermal distribution induce warm air advection over and off the Algerian coast towards eastern Spain. At the same time at middle levels, a positively tilted short wave can be seen over the Iberian Peninsula extending to the southwest and showing two embedded closed lows with cold cores (see Fig. 5b, for 500 hPa). A weak negatively tilted ridge is observed to the east of the Balearics at this level. At 250 hPa (Fig. 5c), three jet-streaks are identified, related to the trough structure.

During next hours, the system at upper levels evolves slowly, driven principally by the positive vorticity advection, that also deeps and extents the surface African depression as seen from Fig. 6a. The trough tilts negatively without significant translation, shifting coherently with the upper levels jets (Fig. 6b, c).

The southerly flow observed on Fig. 5b crosses over the Atlas mountains (Fig. 1), inducing a pressure redistribution at surface with a lee trough off the Algerian coast and its corresponding relative high upstream of the Atlas. This effect is notable at 1200 UTC (Fig. 5a) and has also been observed and numerically simulated by Ramis et al. (1998), obtaining a great contribution of the Atlas to the intensification of the easterly moist flow towards the Spanish Mediterranean coast.

In order to describe further the synoptic conditions that built up the convective environment over eastern Spain, back trajectories for discrete air parcels were calculated. Back trajectories provide information about the path of the air masses. The trajectories are calculated under the assumption of isentropic motion, and therefore the method provides information about the vertical motion of the air parcels through knowledge of the isentropic surfaces topographies.

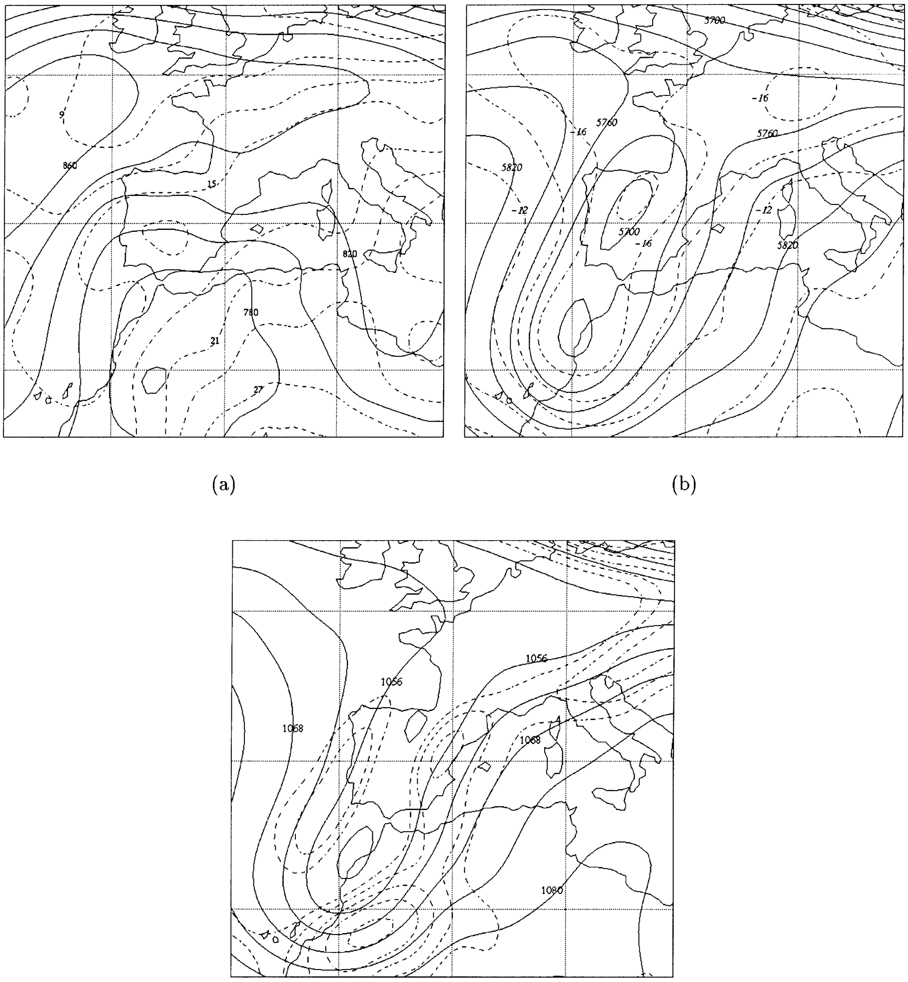

(a) (b)

(c)

Fig. 5. Synoptic situation at 1200 UTC September 28th, 1994 from ECMWF analyses data. At (a) 925 hPa and (b) 500 hPa, geopotential height (gpm) in solid line and temperature (°C) in dashed line. At (c) 250 hPa, geopotential height (gpdam) in solid line and horizontal wind speed in dashed line (contour interval is 5 ms^{-1} starting at 25 ms^{-1}

Following the methodology described in Duquet (1964), values of geopotential, temperature and horizontal wind components on several isentropic surfaces are obtained by interpolation of data from the available isobaric surfaces. Values of the fields at any given time step are determined by linear interpolation between the 6 hours apart ECMWF analyses. Back trajectories are calculated by integrating backward in time the kinematic formulas, where the acceleration term is determined from the Montgomery potential function through application of the equations of motion in isentropic coordinates. A full description of the method can be found in Alarcón (1993).

Figure 7 shows the 3 days back trajectories of several parcels located over the Spanish Mediterranean coast on the 310 K isentropic surface. The parcels exhibit a trajectory originating to the south-southwest. Its vertical position shows that there is a general upward motion over the western Mediterranean, associated with the evolving upper levels trough. That history of the air masses is in agreement with the findings of Tudurí and Ramis (1997), which show that most of the torrential rainfalls in the Balearic zone are produced with warm air in all the troposphere. In addition, at low levels (not shown) the parcels come from the southern part of the western Mediterranean while experiencing a notable lifting along its path, in agreement with the previously noted warm air advection towards the eastern flank of the Iberian Peninsula. Both the trajectory of low-levels parcels, which follow a long path over the warm Mediterranean, and that of the medium-level parcels, which have

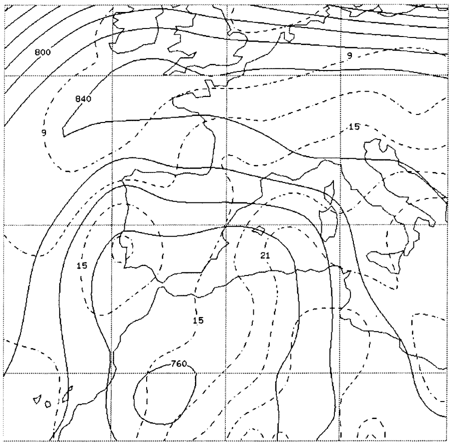

(a)

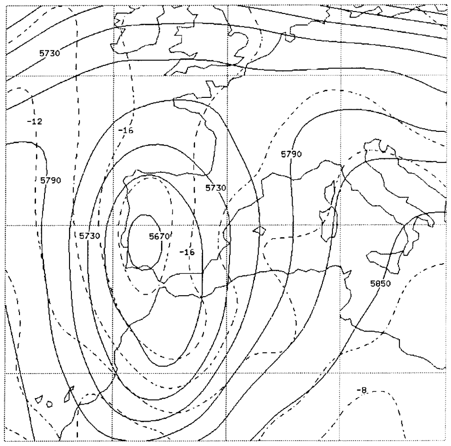

(b)

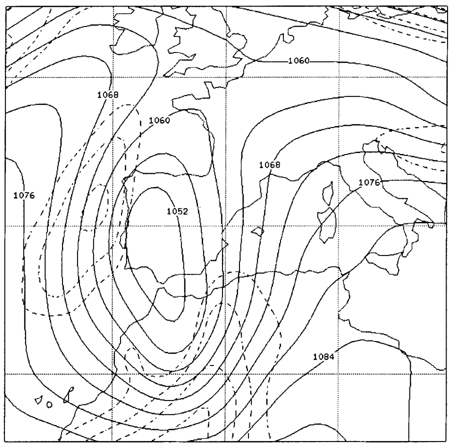

Fig. 6. As in Fig. 5 but at 0600 UTC September 29th, 1994

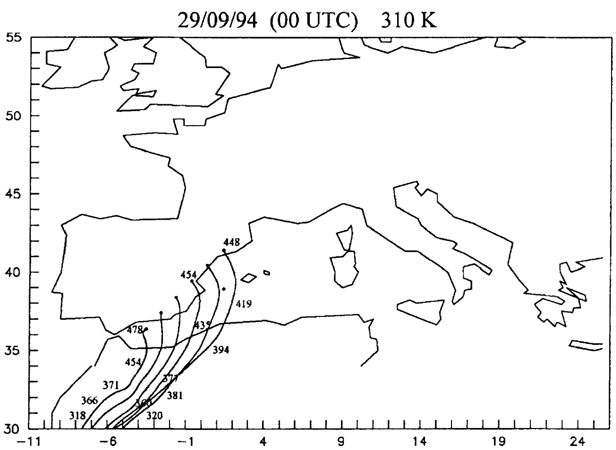

Fig. 7. 3-days back trajectories starting at 0000 UTC September 29th of some parcels located over eastern Spain on the 310 K isentropic surface. Labels indicate height in dam

their roots over the Atlantic, favour high values of precipitable water over the western Mediterranean.

2.2 Remote Sensing Data

Meteosat infrared pictures in Fig. 3a and b show the evolution of the convective systems at the early hours of their development. At 0600 UTC September 28th (Fig. 3a), a cloudy band is observed over the western Mediterranean and eastern Iberian Peninsula. Some convective cells affect eastern Mallorca and an incipient convective development is identified over the Alboran Sea. This latter convective system moved to the northeast very slowly towards the Balearic channel, while another one was developing to the south of the Balearics. Both systems became stronger during the morning of the 28th and met to the south of the Balearic channel, as shown in Fig. 3b. The western one evolved over the Valencian coast during the subsequent hours, whereas the eastern one followed a path along the Balearics and eastwards. The rainfall produced by both systems over the sea is not completely captured by existing observations. Even clear evidences of the precipitation produced by the western convective system are observed on the Valencian radar images, no observation about the precipitation produced by the eastern system is available due to the absence of radar coverage over the Balearic zone.

The rainfall estimated by the Valencia radar can be seen in Fig. 4. The southwest region on Fig. 4 remains sheltered by the prominent mountains of southern Valencia, but the Balearic channel and northern Valencia areas are well covered. A signal over land close to the coastline is observed near the Valencia city (at the centre of the picture) with values exceeding 40 mm. A stronger signal exceeding 80 mm is found to the north, being just partially captured by raingauge available data (Fig. 2). Therefore, although there appear some quantitative differences inland between radar images and raingauges measures, spatial structures over land are fairly similar, and radar signal over the sea can be trustly treated. Three important centres are observed over the sea: the first one to the south with values up to 100 mm, another one to the west, next to the Valencian coast and achieving 120 mm, and an elongated shaped third one to the northeast, achieving values up to 180 mm. The radar derived hourly rainfall sequence (not shown), reveals that the system evolves northwards. It produced the southern and western precipitation centres during the afternoon of the 28th, and then the northeastern one at the early hours of September 29th. A particular issue of this case is the large amount of precipitation fallen over the sea, between the Balearics and mainland Spain. The mechanisms leading to such rainfall will be investigated through numerical experiments.

3. Numerical Model

The numerical model used to perform the simulations was the short range forecasting hydrostatic model Hirlam, described in a documentation manual by Källén (1996). The model was developed as an international co-operative project and is currently used by several european meteorological services.

A geographically oriented Arakawa-C horizontal grid and 31 p-σ hybrid vertical levels (the same as ECMWF model) have been used. A two time level, three-dimensional semi-Lagrangian and semi-implicit integration scheme (McDonald and Haugen, 1993) is used to allow long timesteps, of about 7–10 minutes for 0.3° grid length, without growing noise in forecast fields. The prognostic variables of the model are surface pressure, horizontal wind, temperature, specific humidity and cloud water. The horizontal diffusion is calculated using a sixth-order implicit operator which is applied on all prognostic variables, except on cloud water. Furthermore, diffusion on temperature and specific humidity is applied on isobaric surfaces (quasi-horizontal) to avoid unrealistic heating and moistening at orographic slopes. Vertical fluxes of momentum, sensible heat and moisture, caused by turbulence, as well as surface fluxes, are parameterized following Louis (1979). A force-restore method is used to calculate soil temperature and humidity over land and it is initialized using climatological data, whereas for the sea surface temperature a climatological monthly mean value is used and kept constant during the simulations. Long and short wave radiative processes are parameterized following Savijärvi (1990). Condensation and precipitation processes are parameterized by Sundqvist scheme (Sundqvist et al., 1989) which includes microphysics, large scale condensation and convection, the later based on Kuo scheme (Kuo, 1974). Initial conditions are initialized following the Temperton (1988) expression of the original Machenhauer (1977) nonlinear normal mode scheme. On the other hand, the Davies (1976) lateral boundary formulation is used, applying a cosine shaped relaxation function over a 8 point boundary region.

4. Simulations

Experiments have been done over a grid of 194×100 points and horizontal resolution of $0.3° \times 0.3°$ (roughly $30 \times 30\,km^2$), covering a

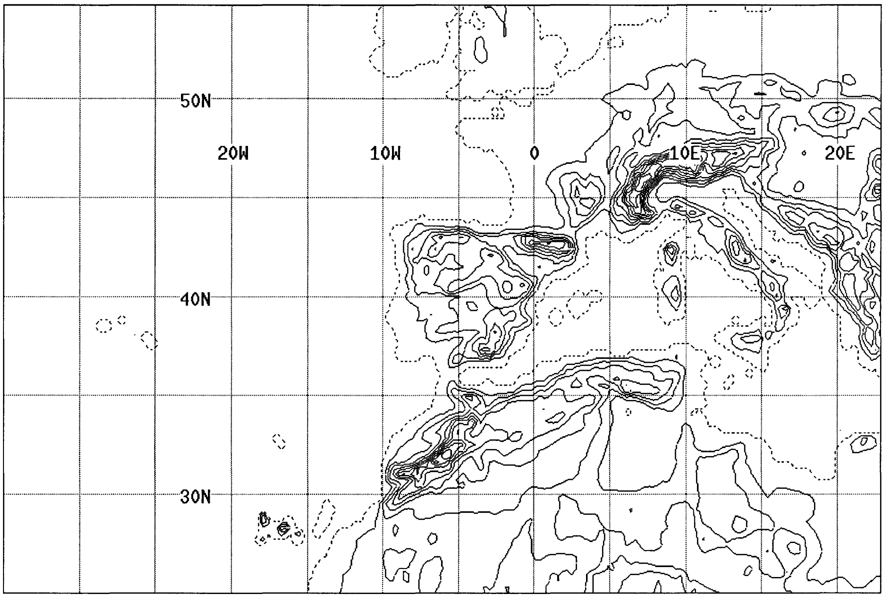

Fig. 8. Model domain and topography used in the complete simulations. Model sea coast-line is shown in dashed line and heigh in solid lines (interval is 250 m starting at 250 m

region of 6000×3000 km^2 approximately (Fig. 8). The orography used to define the vertical levels and to calculate the surface roughness is also presented in Fig. 8. The timestep used for the simulations was 450 s, high enough to save in computational time without compromising the accuracy of the results. Integrations start at 0000 UTC September 28th, 6 hours before the main convection is identified on Meteosat pictures (Fig. 3a), and finish at 0600 UTC September 29th (T + 30 h) after the main precipitation occurs. Uninitialized ECMWF analyses, with 0.75° resolution and available at 00, 06, 12 and 18 UTC, were used as initial and boundary conditions.

4.1 Complete Simulation

A complete simulation (CS) was performed to explore the model capabilities to represent the mechanisms responsible for the notable rainfall of this case.

At 1200 UTC September 28th, after 12 h of simulation, the model forecast at low levels also reproduces the elongated anticyclon over the Atlantic together with the North African low pressure system observed in the ECMWF analyses. Consequently, a cyclonic circulation over the western Mediterranean and the Iberian Peninsula is well marked (Fig. 9a). This circulation is modified by the Algerian Atlas around the African coast by creating a pressure dipole that increases the cyclonic easterly flow to the south of the Balearics and Valencian coast. At 925 hPa, the temperature field reveals a significant gradient off the Algerian coast (Fig. 9a). This temperature structure and the orographically induced lee trough, which drives the air along a notably long path over the sea, result in enhanced warm and moist air advection towards the Valencian coast. Moreover, in agreement with ECMWF analysis (Fig. 5b), the positively tilted binary low centre at 500 hPa is correctly simulated (Fig. 9b). The notable vorticity advection maximum over North Africa, produced by such short trough, induces a rapid deepening of the North African surface low (Fig. 10a).

Next hours, the axis of the upper levels trough tilts negatively, so locating the forcing for surface pressure deepening more to the northeast. At 0600 UTC September 29th (T + 30 h) (Fig. 10b), a blocking inverted Ω-structure (ridge-trough-ridge pattern) as a result of the trough axis rotation is clearly depicted. This rotation, combined with the notable warm air advection at low levels, rebuilds the surface low northwards over the Mediterranean, shifting also northwards the easterly flow and warm advection towards the Spanish coast (Fig. 10a).

The model forecast rainfall is depicted in Fig. 11. Large scale precipitation (not shown) is very weak (only small centers up to 10 mm), so Fig. 11 nearly corresponds to the convective precipitation field. The pattern over the Balearic channel, at the centre of the figure, roughly

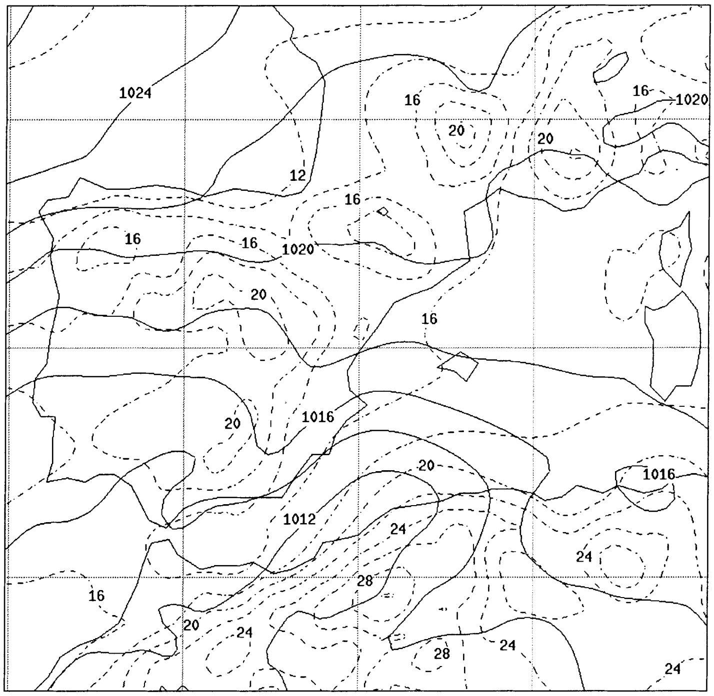

(a)

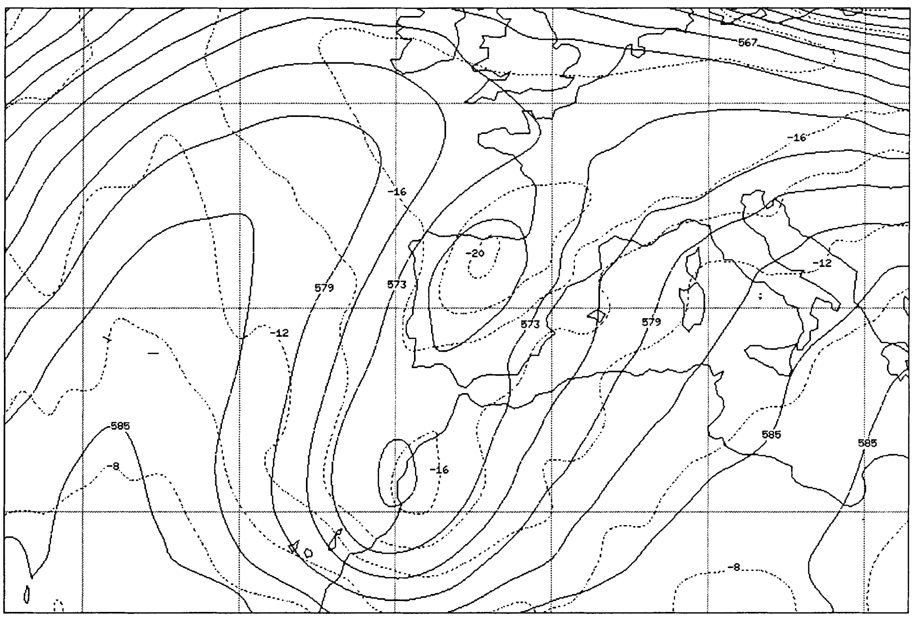

(b)

Fig. 9. Model simulated fields at 1200 UTC September 28th (T + 12 h); a) Zoom over the area of interest of sea-level pressure in hPa (solid lines) and 925 hPa temperature in °C (dashed line), b) Geopotential height in gpdam (solid lines) and temperature in °C (dashed lines) at 500 hPa

resembles that observed in the radar image (Fig. 4). It presents a maximum between the Balearics and mainland Spain, and even an elongation inland over Valencia in a fairly good agreement with the raingauge measured rainfall pattern (Fig. 2). Quantitatively, the precipitation is also well captured by the model, since the 145 mm achieved by the simulation are only a bit lower than the estimated by radar to the north of the island of Eivissa (180 mm, see Fig. 1 for location). Except for the highly local maxima, the amount of rainfall given by the model over

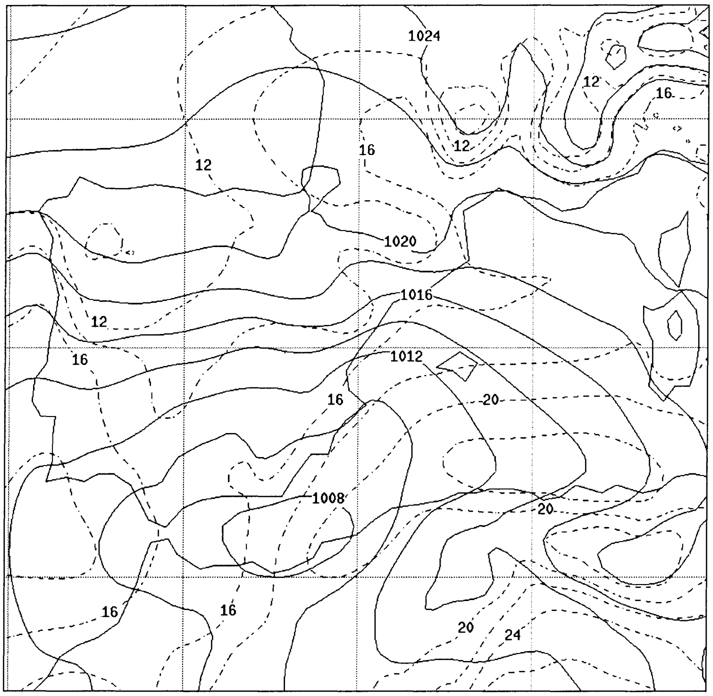

(a)

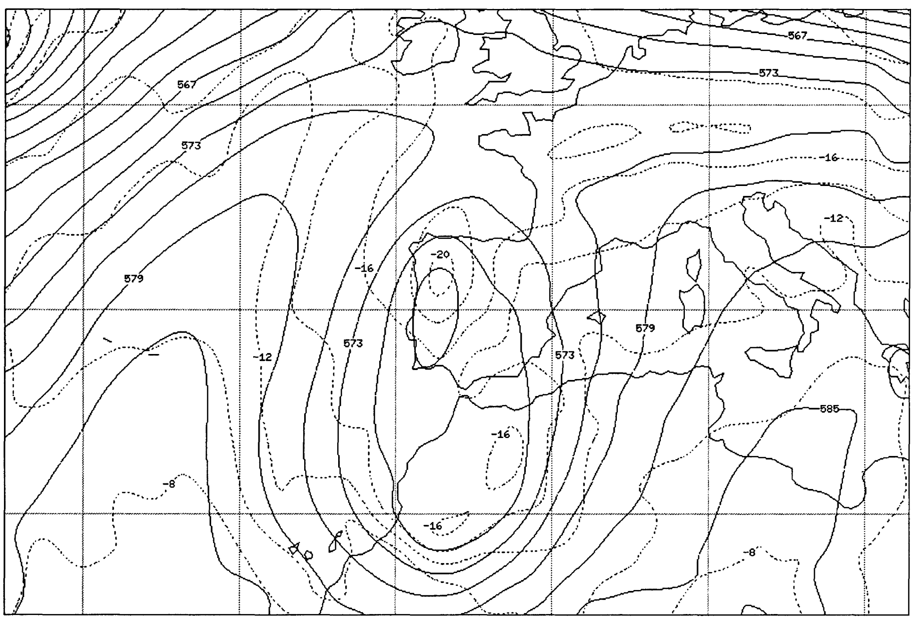

(b)

Fig. 10. As in Fig. 9 but at 0600 UTC September 29th (T + 30 h)

Valencia is also quantitatively correct. The forecast precipitation over Mallorca is very weak (less than 5 mm), contrasting with the substantial raingauge measured rainfall (Fig. 2). The storm producing such precipitation over Mallorca was very small in size and developed very early in the morning of September 28th (Fig. 3a), and therefore the model was in the spin-up time and had little opportunity to do a good job in this case. On the other hand, small and strong precipitation centres are observed to the west of the Atlas. These nuclei seem to reflect spureous precipita-

Fig. 11. Model forecast rainfall at 0600 UTC September 29th (T + 30 h). Continuous contours start at 20 mm with a 20 mm interval, and dashed contour is the 5 mm isohyet

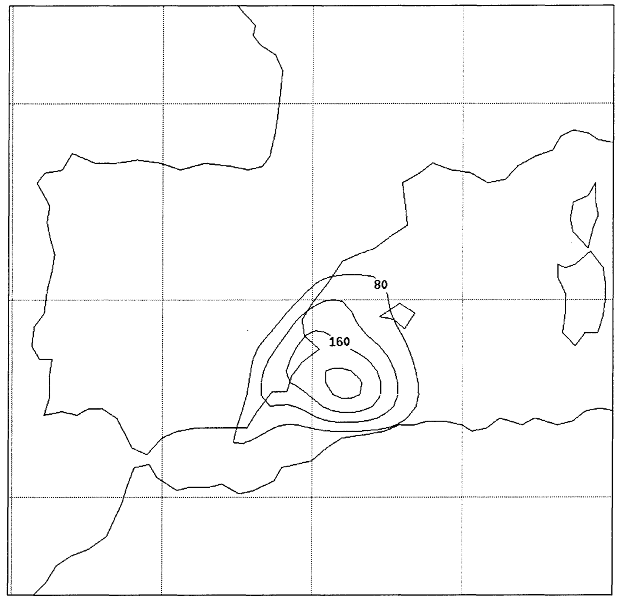

(a)

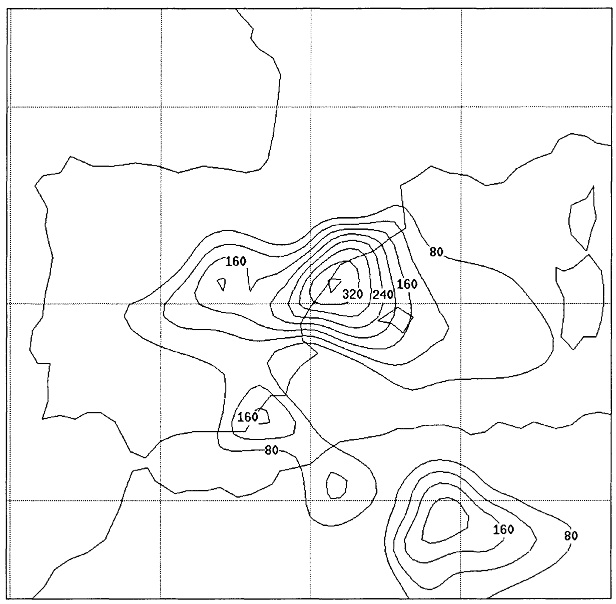

(b)

Fig. 12. Ground Relative Helicity (contour interval is $40\,m^2\,s^{-2}$, starting at $80\,m^2\,s^{-2}$) at a) 1200 UTC September 28th (T + 12 h), b) 0600 UTC September 29th (T + 30 h)

tion produced by the convective scheme through an overestimation of local orographic forcing.

Comparing Meteosat pictures (Fig. 3) with ECMWF analysis and previous model forecasts, it is apparent that convection developed between the trough and the downstream ridge present at middle levels, rather far from the trough forcing region and closer to the ridge. This feature has been observed in several cases of torrential precipitation in the region (e.g., Ramis et al., 1994; Ramis et al., 1998), revealing a weak influence of the classical baroclinic forcing to develop and sustain the convection.

4.2 Diagnostic Study

With the aim of identifying the mechanisms responsible for the convective development in the simulation, some diagnosed fields from the model outputs are examined in this section.

Temperature advection can be easily characterized by using of the Ground Relative Helicity (GRH) (Tudurí and Ramis, 1997). In the present case, the GRH was integrated upwards up to 700 hPa to interpret it in terms of the low tropospheric temperature advection. Figure 12a depicts the GRH field (only positive values) at 1200 UTC September 28th (T + 12 h). An isolated nucleus (with values up to 208 m^2s^{-2}) is observed to the south of the Balearic channel, corresponding to that notable warm advection shown in Fig. 9a. This GRH structure moved slowly over the sea from south to north along the Valencian coastline. It intensified during the afternoon and night and reached Catalonia at 0600 UTC September 29th (T + 30 h) with

$362\,m^2s^{-2}$ at its maximum (Fig. 12b). Together with this GRH maximum, that follows quite precisely the western convective system recognized on Meteosat pictures, positive values are present over the Balearics, where the eastern convective system is identified on Fig. 3b. The presence of such strong GRH signal implies an important warm advection, responsible not only for an inherent static destabilisation of the air column but also for an appreciable upward quasigeostrophic forcing from low levels during all the event.

The evolution of the relative humidity distribution during the case is relevant. At 1200 UTC September 28th (T + 12 h) a moist tongue, with values greater than 90%, is present to the west of the Alboran Sea extending along the Spanish Mediterranean coast at 500 hPa (Fig. 13a). At 0600 UTC September 29th (T + 30 h), the model forecasts high humidity over all the coastal region, reaching values higher than 90% over the Balearic channel, Catalonia and Valencia regions (Fig. 13b). The presence of nearly saturated air at midlevels could explain the high efficiency of the convective systems. It is well known that convective environments with high humidity through most of the troposphere favour high precipitation efficiency (Maddox et al., 1979).

The triggering and driving mechanism of the western convective system, that followed its entire trajectory over the sea, cannot be explained from orographic forcing only (see next section), but it must be searched in different origins. At 0600 UTC September 28th (T + 06 h), when the convective system development is clearly identified on Meteosat picture, two jet streaks are found at high levels on the region of interest (Fig. 14a). These jet streaks are positively interacting in such a way that the right entrance region of the northern one and the left exit region of the southern one are both forcing upward motion around the Alboran Sea, just over the growing convective nucleus identified on Fig. 3a. Indeed, there appears important values of horizontal wind divergence in the overlapping region between both jets, consistent with the associated secondary circulations described by quasigeostrophic theory (e.g., Carlson, 1991). This kinematic signal is present during all September 28th. During the early hours of September 29th, the northern jet advances northward, focusing the upward motion forcing over the Gulf of Valencia (Fig. 14b), where the maximum precipitation rate is either observed by radar and simulated by the model.

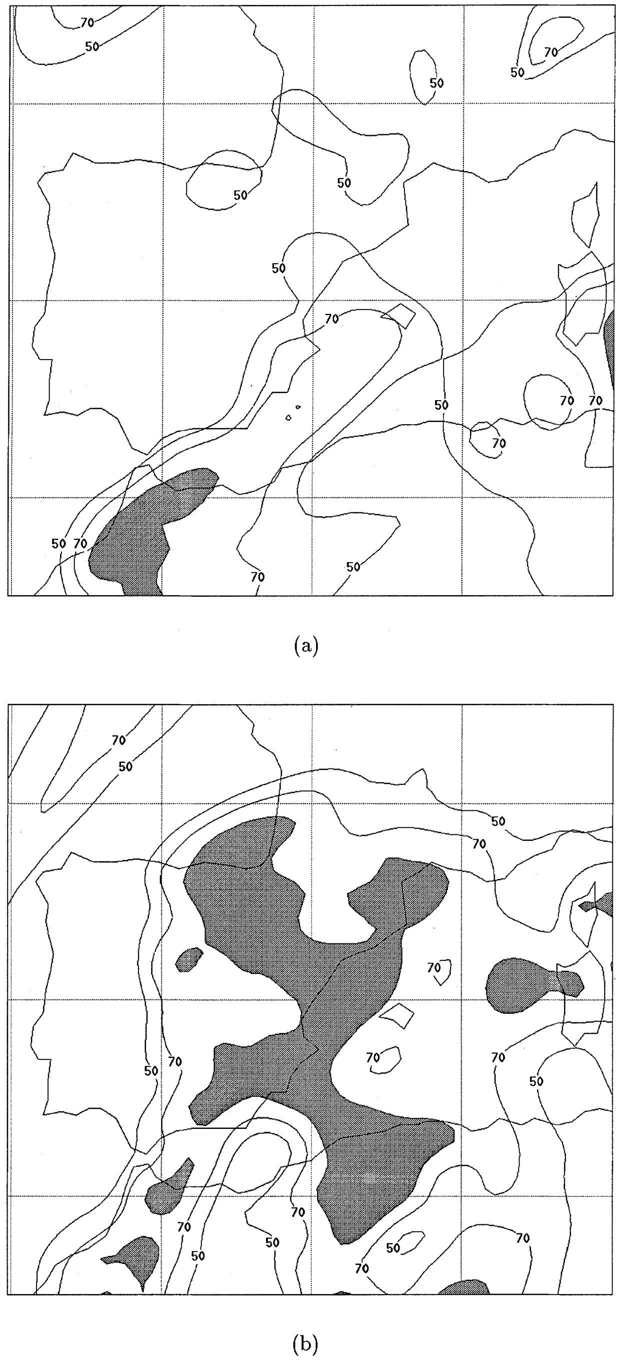

Fig. 13. Relative humidity field at 500 hPa (contour interval is 20% starting at 50%) at a) 1200 UTC September 28th (T + 12 h), b) 0600 UTC September 29th (T + 30 h). Shaded region corresponds to values greater than 90%

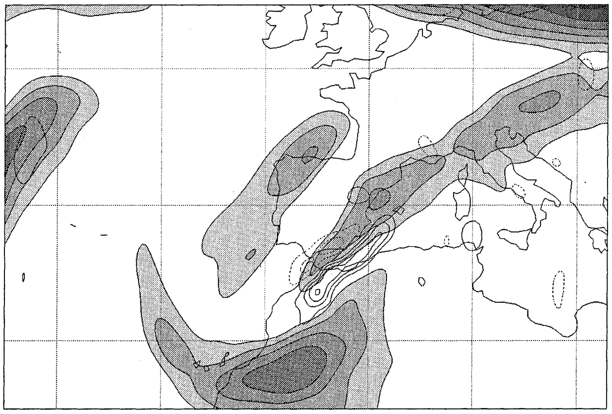

(a)

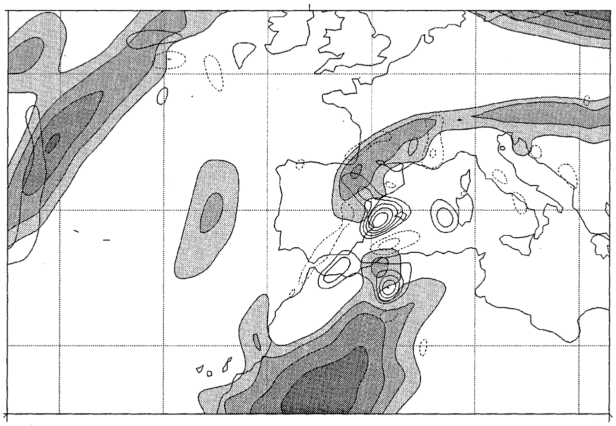

(b)

Fig. 14. Horizontal wind isotachs (shaded) at 250 hPa (contour interval is $5\,\mathrm{m\,s^{-1}}$, starting at $25\,\mathrm{m\,s^{-1}}$) and horizontal wind divergence at 250 hPa (contour interval is $3.10^{-5}\,\mathrm{s^{-1}}$ starting at $3.10^{-5}\,\mathrm{s^{-1}}$ in continuous line, and $-3.10^{-5}\,\mathrm{s^{-1}}$ starting at $-3.10^{-5}\,\mathrm{s^{-1}}$ in dashed line), at a) 0600 UTC September 28$^{\mathrm{th}}$ (T + 06 h) and b) 0200 UTC September 29$^{\mathrm{th}}$ (T + 26 h)

Consistent with the jet-induced upward forcing features, the model diagnoses an upward vertical velocity column beneath, throughout the troposphere (Fig. 15a). During the event, this structure moved slowly north-eastward along the Balearic channel to Catalonia, following the area where the previously identified forcing mechanism is strongest. A time sequence of forecast fields (not shown) illustrates a close correspondence between the vertical plume of upward motion and the area where the model develops convection. In addition, the remarkable low levels water vapor flux convergence (Fig. 15) allows the continuous feeding of the system with moisture rich air.

As discussed previously, the Atlas mountains seems to have played a certain role in this case. The cyclogenetic effect over the Mediterranean, as a result of its interaction with the middle levels southerly flow, acts in favour of the warm and moist air advection towards eastern Iberian Peninsula. Next sub-sections are devoted to the quantification of the orographic role for the rainfall distribution.

4.3 Non-Topographic Simulation

A non-topographic simulation (NTS), identical to the CS but without topography in the model, was performed. Obviously, the results of this simulation will have still a subtle orographic influence through the initial and boundary conditions, but we interpret the differences between CS and NTS as the closest description of the actual orographic effect on the atmosphere that can be managed.

The main differences between both simulations appear at low levels. Figure 16 shows the effect of orography on the sea level pressure. In the study region, the field reflects two clear pressure dipoles across the Algerian Atlas and the Iberian Peninsula, with south-north and southeast-northwest axis, respectively. Combination of the Atlas induced negative center and the Iberian positive one results on an enhancement of the northeasterly flow over the south of the Balearic channel. The absence of the Algerian coast dipolar deformation in the NTS sea level pressure field (Fig. 17a) points out the actual shape of the North African low. In the following hours, positive vorticity advection by the upper levels trough (not shown for NTS but quite similar to that in CS, Fig. 9b) and low levels warm advection drive the north african surface low to the northeast. Such displacement shifts the focus of easterly flow towards northern Valencia and Catalonia (Fig. 17b). The 925 hPa temperature field is also slightly modified; in particular, a smaller thermal gradient appears over eastern Spain.

The weakening of the temperature gradient and the easterly flow over the Mediterranean produces smaller temperature advection towards the Valencian coast. Figure 18 shows the GRH field for the NTS experiment. Weaker structure

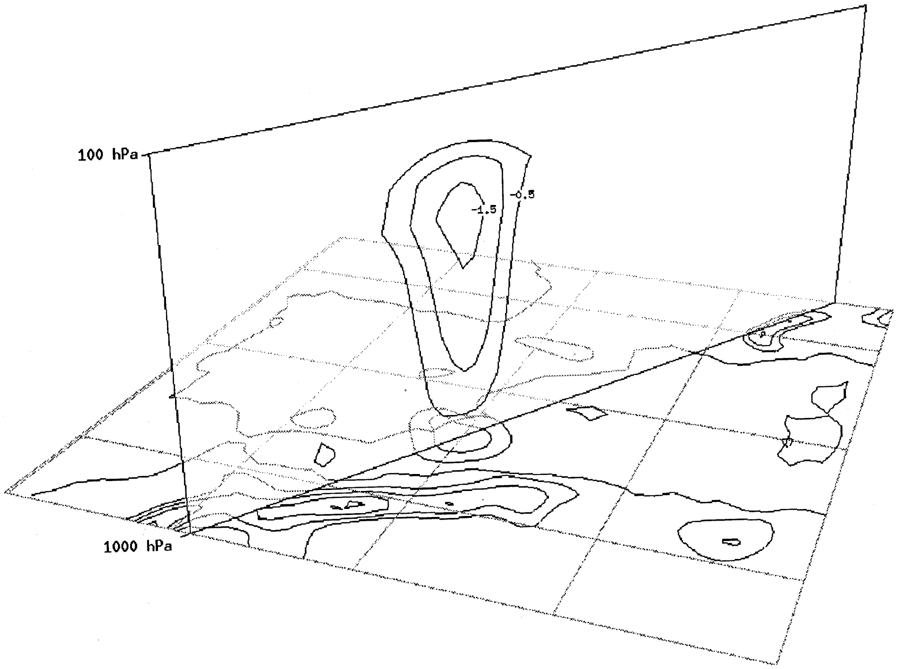

(a)

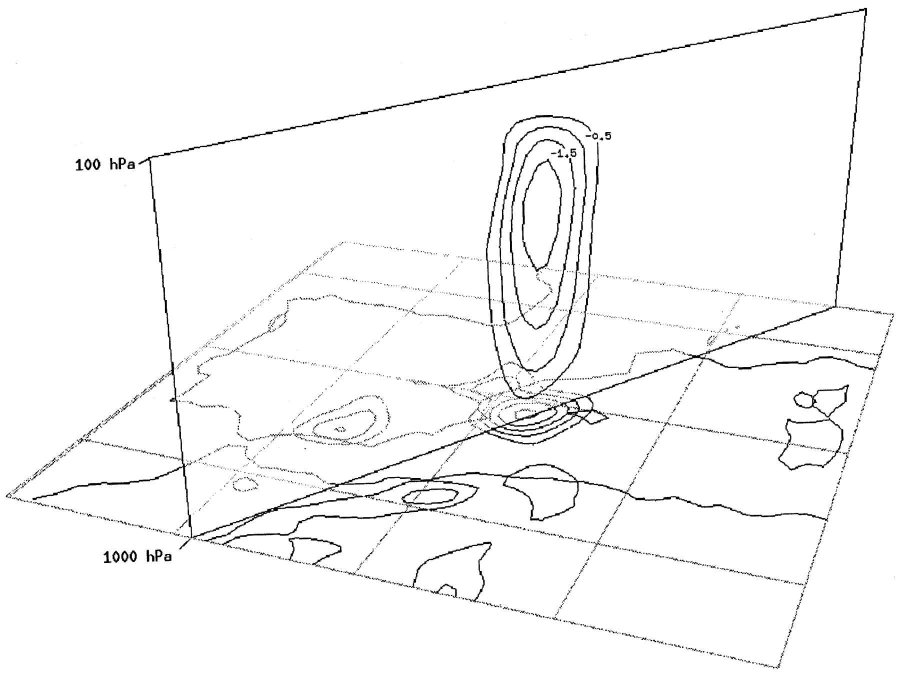

(b)

Fig. 15. Cross section showing upward vertical velocity (contour interval is $-0.5\,\mathrm{Pa\,s^{-1}}$, starting at $-0.5\,\mathrm{Pa\,s^{-1}}$); and horizontal water vapor flux convergence between 1000 and 700 hPa (contour interval is $0.5\,\mathrm{g\,m^{-2}\,s^{-1}}$, starting at $0.5\,\mathrm{g\,m^{-2}\,s^{-1}}$) at a) 1200 UTC September 28th (T + 12 h), b) 0600 UTC September 29th (T + 30 h)

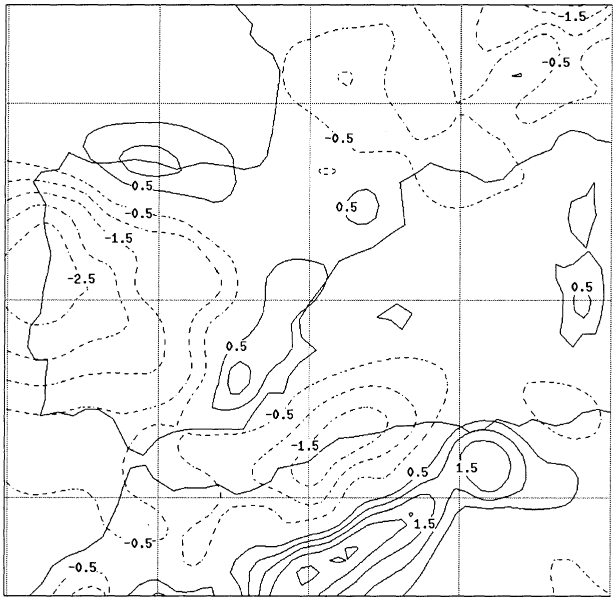

Fig. 16. Sea level pressure difference field between complete (CS) and non topographic (NTS) simulations at 1200 UTC September 28th (T + 12 h) (contour interval is 0.5 hPa starting at 0.5 hPa in continuous line, and −0.5 hPa starting at −0.5 hPa in dashed line)

than in CS (Fig. 12) appears, but still an isolated signal is obtained over Balearic channel and Spanish coast during the event. The greatest values in the nucleus are 171 m^2s^{-2} at 1200 UTC September 28th (T + 12 h) (against 208 m^2s^{-2} in the CS), and 194 m^2s^{-2} at 0600 UTC September 29th (T + 30 h) (against 362 m^2s^{-2} in the CS).

The triggering and focusing mechanism for convection found at upper levels in CS is also detected and even better isolated in the NTS experiment. In Fig. 19, the presence of a jet streak along the northeastern Spanish coast is forcing upward motion through horizontal wind divergence. The jet right entrance region is contributing, in both CS and NTS, to the notable upward motion plume previously shown (Fig. 15). At 1200 UTC September 28th (T + 12 h) (Fig. 19a) the signal of jet-level divergence is located over the GRH nucleus identified at low levels (Fig. 18a). Thus, low and upper levels forcing coincide on the same column, favouring the convection to be maintained during the simulation. At 2000 UTC (T + 20 h) this signal has evolved to the north, over and to the west of the Balearics (Fig. 19b). On the other hand, another important signal of upper levels divergence appears over the Atlas, just between the

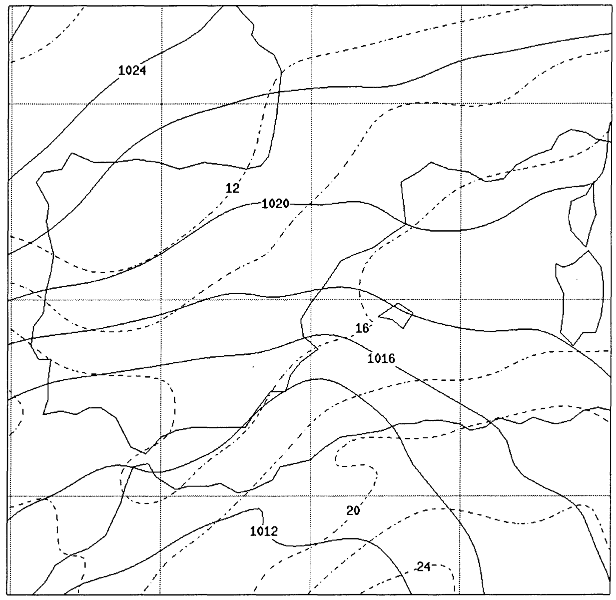

(a)

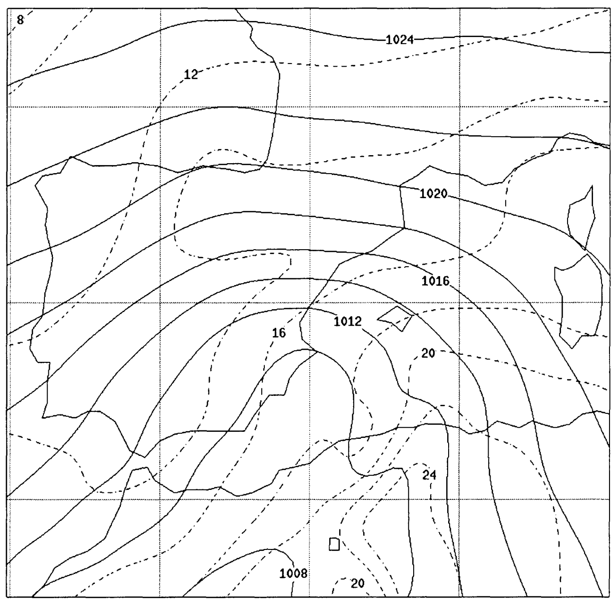

(b)

Fig. 17. Non topographic simulation. Sea level pressure in hPa (solid lines) and 925 hPa temperature in °C (dashed lines) at a) 1200 UTC September 28th (T + 12 h), and b) 0600 UTC September 29th (T + 30 h)

right entrance region of the northern jet's tail and the left exit region of the African jet. This interaction causes the triggering of additional convection in the NTS simulation that produces important rainfall over the Algerian coastal zone. This feature, however, is not simulated by CS owing to different jet evolution and structure.

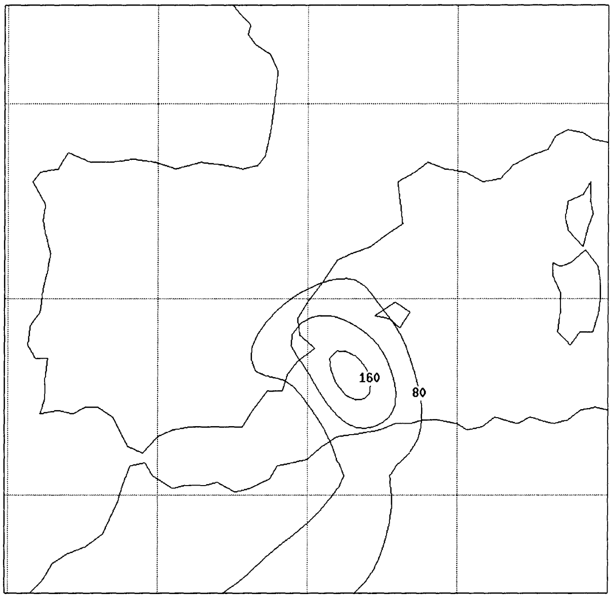

(a)

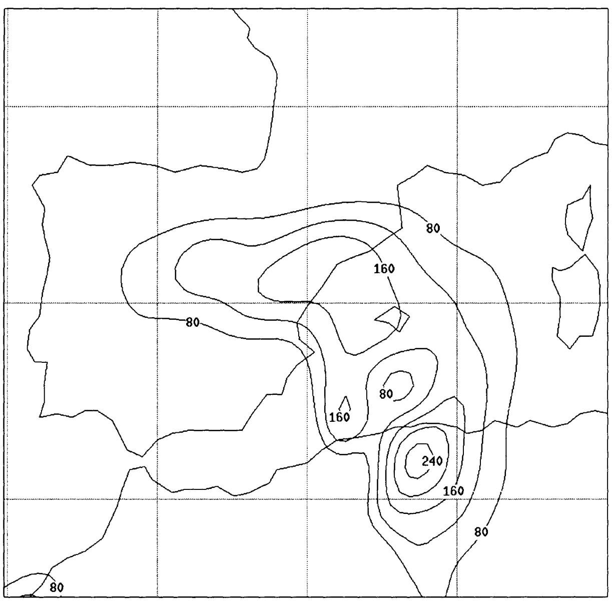

(b)

Fig. 18. Non topographic simulation. Ground relative helicity (contour interval is $40\,m^2\,s^{-2}$ starting at $80\,m^2\,s^{-2}$) at a) 1200 UTC September 28th (T + 12 h) and b) 0600 UTC September 29th (T + 30 h)

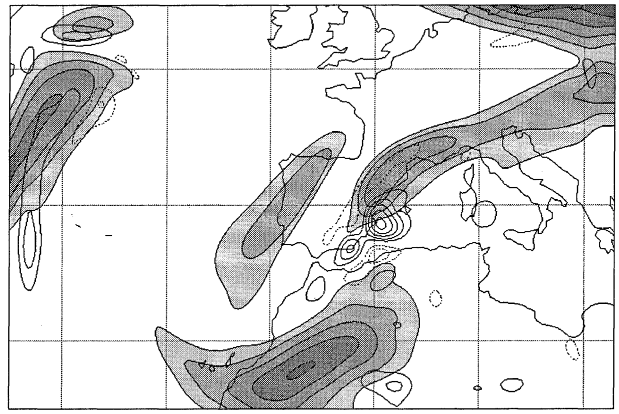

(a)

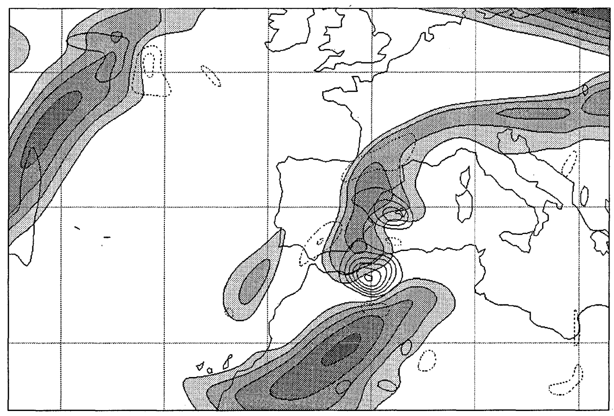

(b)

Fig. 19. Non topographic simulation. Horizontal wind isotachs (shaded) at 250 hPa (contour interval is $5\,m\,s^{-1}$, starting at $25\,m\,s^{-1}$) and horizontal wind divergence at 250 hPa (contour interval is $3.10^{-5}\,s^{-1}$ starting at $3.10^{-5}\,s^{-1}$ in continuous line, and $-3.10^{-5}\,s^{-1}$ starting at $-3.10^{-5}\,s^{-1}$ in dashed line), at a) 1200 UTC September 28th (T + 12 h) and b) 2000 UTC September 28th (T + 20 h)

Figure 20a depicts the accumulated precipitation at 0600 UTC September 29th (T + 30 h). Significant amount of precipitation is observed in the Balearic channel, together with a second maximum over the Algerian coast. The former reaches values greater than 80 mm, which is a very high value compared with previous non-topographic studies in eastern Spain (Ramis et al., 1998; Romero et al., 1998). More than a half of the CS maximum precipitation over the sea (140 mm in Fig. 11) cannot be attributed to mechanisms related, either directly or indirectly, to the orography.

The difference field between CS and NTS rainfall patterns is depicted in Fig. 20b. The negative nucleus over the Atlas and Algerian coast reflects the previously commented convection given by NTS but not by CS. The effect of orographic factor is positive around the Valen-

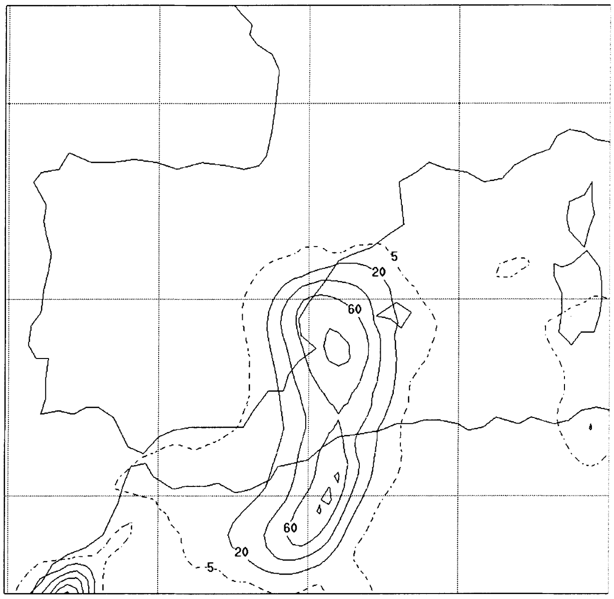

(a)

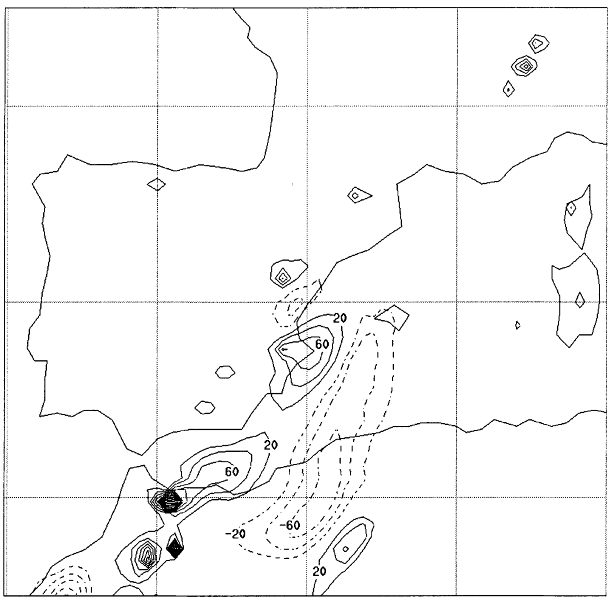

(b)

Fig. 20. a) Accumulated precipitation (continuous lines start at 20 mm with 20 mm interval, and dashed line represents 5 mm) at 0600 UTC September 29th (T + 30 h) for Non topographic simulation (NTS); b) Precipitation difference field between complete (CS) and non topographic (NTS) simulations (contour interval is 20 mm starting at 20 mm in continuous line, and −20 mm starting at −20 mm in dashed line)

cian coast but negative to the east of the Balearic channel. This is a result of the more focused rainfall pattern produced by CS, that not only concentrates precipitation over the Gulf of Valencia and neighbouring lands but displaces the sea precipitation nucleus to the west (compare Figs. 11 and 20a). Although differences over inland Valencia reach values up to 80 mm, the rainfall structure over the sea (where a substantial amount of precipitation has been obtained in both simulations) is very similar. This certainly relativises the importance of the orographic factor which, as previously indicated, has been traditionally highlighted as the most relevant ingredient for the development of torrential rainfalls in eastern Spain (Miró-Granada, 1974).

4.4 Role of the Atlas and Iberian Topography

Despite the unusual upper levels forcing found in this case, the effect of the orography is still important since it accounts for about a half of the precipitation over the area of interest. In the NTS experiment, the roles of the Atlas range and the Iberian Peninsula are both supressed. Therefore, it is not possible from only CS and NTS experiments to isolate the quantitative contribution of each topographic system. Individual contributions together with their interaction can be obtained following the factor separation technique of Stein and Alpert (1993). Two additional simulations were necessary to be performed (Table 1): a first simulation without the African topography (referred to as Iberian Peninsula Simulation, PS), and a second one designed without European topography (Atlas Simulation, AS). Then, the effects of the factors (Atlas, Iberian Peninsula and the interaction) on any given model output (e.g., precipitation) are calculated as:

1. Effect of the Atlas = AS−NTS
2. Effect of the Iberian Peninsula = PS−NTS
3. Effect of the interaction = CS − (AS+PS) + NTS

Table 1. *Summary of the Numerical Experiments Designed for the Study*

	Topography	
Simulation	Africa	Europe
CS	YES	YES
AS	YES	NO
PS	NO	YES
NTS	NO	NO

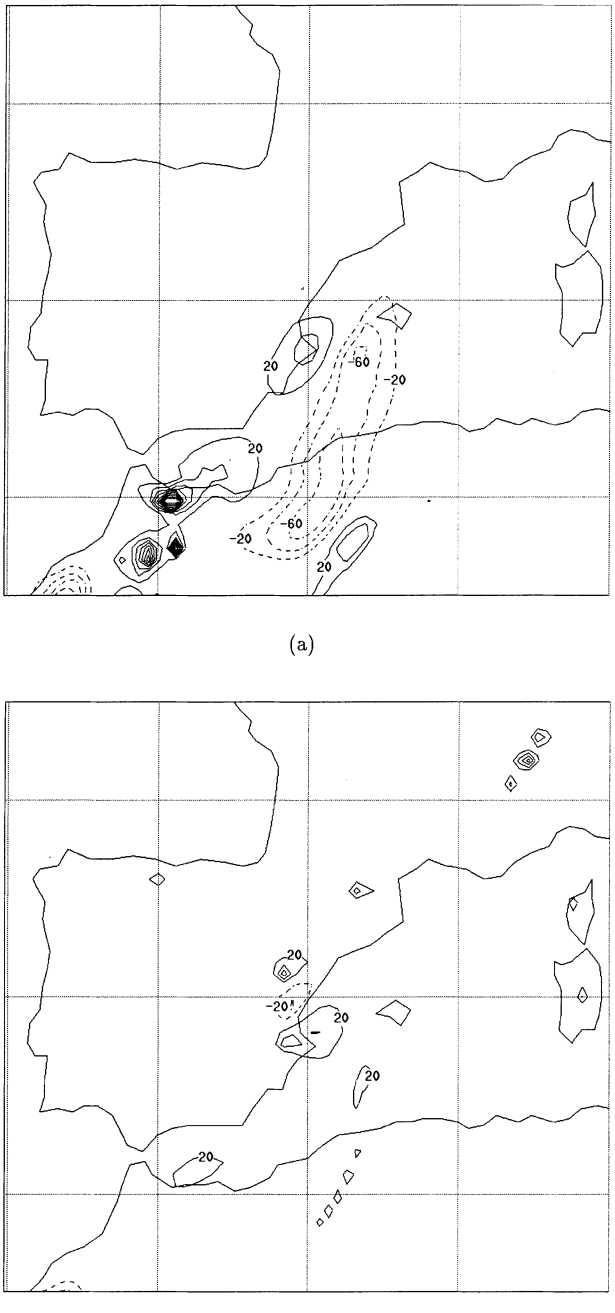

Fig. 21. Effect of a) Atlas (AS-NTS), and b) Iberian (PS-NTS) orography on the accumulated precipitation at 0600 UTC September 29th (T + 30 h). Contour interval is 20 mm starting at 20 mm in continuous line, and −20 mm starting at −20 mm in dashed line

Note that the sum of these contributions is the total effect of the orography, CS−NTS.

Figure 21 depicts the effects of Atlas and Iberian Peninsula on the accumulated precipitation at 0600 UTC September 29th (T + 30 h). The effect of the Atlas (Fig. 21a) exhibits a nearly identical pattern to the total topographic effect (Fig. 20b). About the Balearic channel, the effect of the Atlas is a spatial redistribution of the precipitation field in such a manner that more than 40 mm from the South of the Balearics are shifted downstream to the Valencian coast. Furthermore, Fig. 21a reveals that the negative nucleus over Algeria seen on Fig. 20b is entirely due to the Atlas range.

The effect of the Iberian peninsula orography, particularly the Valencian mountains, is essentially positive and local (Fig. 21b). In the area of interest, this effect is a focalisation of more than 40 mm of rainfall over southern Valencia. This is consistent with the findings of Romero et al. (1999), where it is shown that northeasterly flows induce a substantial rainfall enhancement over south Valencia upslopes. The interaction effect (not shown) is weak with a negative center over the Valencian coast, that acts against the additive effects of the Atlas and Iberian Peninsula. Therefore, both orographic systems affect the precipitation field rather independently.

On the other hand, an inspection of the contributions of these factors to the sea level pressure field reveals that the Algerian and Iberian dipoles previously identified on the total effect (Fig. 16), are fully produced by the Atlas range and Iberian plateau, respectively.

5. Conclusions

A case of deep convection producing heavy precipitation over the western Mediterranean has been presented and numerically studied, trying to ascertain the mechanisms leading to its development. A broad overview of the case has shown that the typical pattern of low levels easterly warm and moist air advection towards the Spanish coast was present. At upper levels, the synoptic pattern was characterized by a short deep trough to the Southwest of Spain and a negatively tilted ridge to the Northeast of the Balearics. On the other hand, satellite pictures have shown the presence of deep convection from the early hours of September 28th and have helped to identify two main systems evolving over the region. The radar images obtained from Valencia reveal a great amount of precipitation fallen over the sea, at the Balearic channel.

Numerical simulations have been done using Hirlam mesoscale model to assess the role of orographic forcing in this case. A first complete simulation has shown the capability of the model to predict both spatial and quantitative details of the precipitation field reasonably well. The results show that, in addition to the synoptic lower levels forcing pattern already observed in previous torrential rainfall cases, the higher levels dynamical forcing associated with a couple of jet-streaks appears to be crucial for the development of convection. A non-topographic simulation has shown the moderate influence of the orography on this case. In other similar events (in precipitation and synoptic situation) occurred in eastern Spain, quite all the convective rainfall has a topographic origin. In this case, approximately a half of the precipitation about the Valencian area can be attributed to the orography through two distinct main contributions: a local rainfall enhancement by the Valencian mountains, and a spatial redistribution of precipitation over the Balearic channel by the remote action of the Atlas range.

Although no strict quantitative isolation of the contribution of the higher levels forcing has been done, clear evidences of its decisive role in the development and driving of the convection have been presented. Such forcing is attributed to the interacting jet-streaks concept, ageostrophic secondary circulations, and vertical velocity field. Such type of results are potentially important for the regional forecasters, since the influence of the higher levels dynamics, not always present in heavy rainfalls in eastern Spain, is stressed. Normally, most of previous studies dealing with heavy precipitations in the Spanish Mediterranean basin have paid more attention to low levels processes, since these usually play a key role in the development, focalisation and maintenaince of deep convection.

Acknowledgements

Satellite pictures were provided by Prof. J. L. Casanovas from the Universidad de Valladolid. Radar information, raw precipitation data and ECMWF meteorological fields were provided by the Instituto Nacional de Meteorologia (INM) of Spain. The HIRLAM System was developed by the HIRLAM Project group, a cooperative project of the national weather services in Denmark, Finland, Iceland, Ireland, the Netherlands, Norway, Spain and Sweden. This work has been sponsored by DGICYT PB94-1169-C02-2 grant.

References

Alarcón, M., 1993: *Simulation of Long-Range Atmospheric Transport and Deposition of Substances at the Western Mediterranean: Trajectory Models and Diffusion-Deposition Processes* (in Catalan). Avda. Diagonal, 647. 08028 Barcelona. Spain: Ph.D. thesis, University of Barcelona.

Carlson, T. N., 1991: *Mid-Latitude Weather Systems*. London: Harper Collins, 507 pp.

Davies, H. C., 1976: A lateral boundary formulation for multi-level prediction models. *Quart. J. Roy. Meteor. Soc.,* **102**, 405–418.

Doswell III, C. A., Brooks, H., Maddox, R., 1996: Flash flood forecasting: An ingredients-based methodology, *Wea. Forecasting,* **10**, 560–581.

Doswell III, C. A., Ramis, C., Romero, R., Alonso, S., 1998: A diagnostic study of three heavy precipitation episodes in the western Mediterranean. *Wea. Forecasting,* **13**, 102–124.

Duquet, R. T., 1964: *Data Processing for Isentropic Analysis*. Hanscom AFB, MA 01731: Tech. Rep. num. 1, contract (30-1)-3317, Air Force Cambridge Research Laboratories.

Font, I., 1983: *Climatology of Spain and Portugal* (in Spanish) Apartado 285, 28071, Madrid. Spain: Instituto Nacional de Meteorología, 296 pp.

García-Dana, F., Font, R., Rivera, A., 1982: *Meteorological Situation During the Heavy Rainfall Event in Eastern Spain in October 1982* (in Spanish). Apartado 285, 28071, Madrid: Instituto Nacional de Meteorología.

Källén, E., 1996: *Hirlam Documentation Manual*. Available from SMHI S-60176 Norrkoping. Sweden.

Kuo, H., 1974: Further studies of the parameterization of the influence of cumulus convection on large-scale flow. *J. Atmos. Sci.,* **31**, 1232–1240.

Llasat, M. C., 1987: *Heavy Rain Events in Catalonia: Genesis, Evolution and Mechanism* (in Spanish). Avda. Diagonal, 647. 08028 Barcelona. Spain: Ph.D. thesis, University of Barcelona.

Louis, J. F., 1979: A parametric model of vertical eddy fluxes in the atmosphere. *Bound.-Layer Meteor.,* **17**, 187–202.

Machenhauer, B., 1977: On the dynamics of gravity oscillations in a shallow water model with applications to normal mode initialization. *Beitr. Atmos. Phys.,* **50**, 253–271.

Maddox, R. A., Chappell, C. F., Hoxit, L. R., 1979: Synoptic and meso-α scale aspects of flash flood events. *Bull. Amer. Meteor. Soc.,* **60**, 115–123.

McDonald, A., Haugen, J., 1993: A two time level, three-dimensional semi-lagrangian and semi-implicit grid point model II. extension to hybrid coordinates. *Mon. Wea. Rev.,* **121**, 2077–2087.

Miró-Granada, J., 1974: Catastrophic flash floods in the western Mediterranean (in French). *AMS-AISH Public.,* **12**, 119–132.

Ramis, C., Jansá, A., Alonso, S., Heredia, M. A., 1986: Convection over the western Mediterranean: Synoptic study and remote observation (in Spanish). *Rev. Meteorología,* **7**, 59–82.

Ramis, C., Llasat, M. C., Genovés, A., Jansá, A., 1994: The october 1987 floods in Catalonia: Synoptic and mesoscale mechanisms. *Meteor. Appls.,* **1**, 337–350.

Ramis, C., Romero, R., Homar, V., Alonso, S., Alarcón, M., 1998: Diagnosis and numerical simulation of a torrential precipitation event in Catalonia (Spain). *Meteorol. Atmos. Phys.,* **69**, 1–21.

Riosalido, R., 1990: Characterization of mesoscale convective systems by satellite pictures during PREVIMET MEDITERRANEO-89 (in Spanish). In: *Segundo Simposio Nacional de Predicción*, Apartado 285, 28071, Madrid, pp. 135–148. Instituto Nacional de Meteorología.

Romero, R., Ramis, C., Alonso, S., 1997: Numerical simulation of an extreme rainfall event in Catalonia: Role of orography and evaporation from the sea. *Quart. J. Roy. Meteor. Soc.,* **123**, 537–559.

Romero, R., Ramis, C., Alonso, S., Doswell III, C. A., Stensrud, D., 1998: Mesoscale model simulations of three heavy precipitation events in the western Mediterranean. *Mon. Wea. Rev.,* **126**, 1859–1881.

Romero, R., Ramis, C., Guijarro, J. A., 1999: Daily rainfall patterns in the Spanish Mediterranean area: An objective classification. *Int. J. Climatol.,* **19**, 95–112.

Savijärvi, H., 1990: Fast radiation parameterization schemes for mesoscale and short range forecast models. *J. Appl. Meteor.,* **20**, 437–447.

Stein, U., Alpert, P., 1993: Factor separation in numerical simulations. *J. Atmos. Sci.,* **50**, 2107–2115.

Sundqvist, H., Berge, E., Kristánsson, J., 1989: Condensation and cloud parameterization studies with a mesoscale numerical weather prediction model. *Mon. Wea. Rev.,* **117**, 1641–1657.

Temperton, C., 1988: Implicit normal mode initialization. *Mon. Wea. Rev.,* **116**, 1013–1031.

Tudurí, E., Ramis, C., 1997: The environments of significant convective events in the western Mediterranean. *Wea. Forecasting,* **12**, 294–306.

Authors' addresses: V. Homar, C. Ramis, R. Romero and S. Alonso, Meteorology Group, Departament de Física, Universitat de les Illes Balears, Palma de Mallorca, Spain; J. A. García-Moya, Instituto Nacional de Meteorología, Madrid, Spain; M. Alarcón, Departament de Física i Enginyeria Nuclear, Universitat Politécnica de Catalunya, Vilanova i la Geltrú, Barcelona, Spain.